***SI Appendix* for:**

Persistence of the permeability transition pore in human mitochondria devoid of ATP synthase

Joe Carroll[1], Jiuya He[1], Shujing Ding, Ian M. Fearnley and John E. Walker[2]

Medical Research Council Mitochondrial Biology Unit, University of Cambridge, Cambridge Biomedical Campus, Hills Road, Cambridge CB2 0XY, United Kingdom

[1]Equal contributions

[2]To whom correspondence should be addressed. e-mail: walker@mrc-mbu.cam.ac.uk

Materials and Methods

Gene Disruption. HAP1-WT cells were obtained from Horizon Discovery (Cambridge, U.K.). Human *ATP5F1D*, encoding the δ-subunit of ATP synthase was disrupted in HAP1-A12 cells (1) by CRISPR-Cas9 technology (2). *ATP5F1D* has 4 exons (*SI Appendix*, Fig. S6) and is located on chromosome 19 which contains a fragment of chromosome 15 in HAP1 cells (3). However, this rearrangement does not affect the expression of the δ-subunit and its assembly into ATP synthase (1). *ATP5F1D* was targeted with gRNA GCTGGTCGTGGTGCATGCAG. The targeted gene region was amplified by PCR with the forward and reverse primers TCACTTTCTGGACCCCAGTACTCA and CGCACACCTTGCCCGAC, and this G-C rich region in *ATP5F1D* was sequenced by dGTP chemistry (Source Bioscience). The sequence revealed that a single base pair deletion had been introduced into exon II, causing a frame shift of codons 89-98, and producing a termination codon at position 99 (*SI Appendix*, Fig. S7).

General Methods. Oxygen consumption rates of cells were measured in a Seahorse XF^{e}24 instrument (Agilent). Measurements were made with cells in Seahorse XF assay medium (Agilent) plus 2 mM glucose and 1 mM pyruvate, with pH re-adjusted to 7.4, and temperature

at 37°C. Oligomycin, carbonyl cyanide-4-(trifluoromethoxy)-phenylhydrazone, and a mixture of rotenone and antimycin A, were introduced successively at final concentrations of 1 μM, 0.5 μM and 0.6 μM each, respectively. Oxygen (O_2) consumption rate was normalized to cell number by the sulforhodamine B colorimetric assay (4). Antibodies against the δ- and ATP6-subunits were purchased from Abcam (ab97491 and ab219825, respectively). The origins of other antibodies have been described before (5). The relative copy number of mtDNA in HAP1-Δ(c+δ) cells was determined as described before (1), except that the PCR template was 20 ng of total cellular DNA and the reaction volume was 20 μL. DNA was amplified with the TaqMan gene expression master mix and the primer and probe sets Hs02596865_g1 (for *MT-CO2*) and Hs02339796_cn (for *APP*) from Thermo Fisher Scientific.

PTP Assay with Thapsigargin and Ferutinin. PTP opening in intact HAP1 cells was induced with thapsigargin (6) or ferutinin (7), and monitored by the calcein-cobalt assay and mitochondrial TMRM fluorescence as described before (1). The calcein (excitation at 475 and emission at. 560 nm, with a 35 nm span) and TMRM (excitation at 530 nm and emission at 675 nm, with a 75 nm span) fluorescence intensities in cells with or without treatment with thapsigargin or ferutinin were measured in samples of cells using a Nucleocounter NC3000 cell counting fluorescence microscope (ChemoMetec). The fluorescence intensities of individual cells were plotted on 2D scatter plots, versus blue fluorescence intensities for nuclei staining with Hoechst 33342 dye, on the ordinate and abscissa, respectively. The fluorescence intensities for the WT cells, which formed a cluster, were encompassed into the upper two quadrants by orthogonal axes. The axes were placed automatically in the same positions on the experimental scatter plots, and the percentage fraction of cells in each quadrant was recorded by the instrument (see example in *SI Appendix*, Fig. S3). The ratio of the positive percentage (the sums of "the percentage fractions" in the upper two quadrants) from experimentally perturbed and unperturbed control cells is the "relative ratio". The averages of relative ratios

from independent duplicate experiments were plotted on a bar chart. Standard deviations and statistical evaluations by student's t-test were calculated with Excel software.

Mitochondrial Calcium Retention Capacity and Membrane Potential Measurements with Permeabilized Cells. Plasma membranes were permeabilized with high-purity digitonin (Calbiochem) (1). Digitonin was added at 60 μg/ml to a suspension of 20 x 10^6/ml cells in cold DPBS containing 2x cOmplete EDTA-free protease inhibitor cocktail (Roche) and 20 μM EGTA (pH 7.4), and then kept on ice for 10 min with occasional mixing by gentle inversion. The resulting permeabilized cells were washed twice with cold DPBS containing 1x cOmplete inhibitors and 20 μM EGTA (pH 7.4), and then twice in the same wash solution minus EGTA. Portions of cells (60 x 10^6) required for individual analyses were centrifuged and the cell pellets were kept on ice. Mitochondrial CRC was assayed as described before (1) except that exogenous calcium was measured with 0.2 or 0.25 μM calcium green-5N. The effects of bongkrekic acid (Sigma) and carboxyatractyloside (Sigma) on mitochondrial CRC assay, were studied by adding them to the permeabilized cells during the 2 min pre-incubation period at 30°C preceding the assay. Where citrate synthase levels were used for normalization, the activity of citrate synthase was determined in DDM extracts of HAP1-WT and HAP1-Δ(c+δ) cells by the measurement of thionitrobenzoic acid released by the reaction of 5,5-dithiobis-(2-nitrobenzoic acid) with CoA-SH (8). Using the same experimental conditions as the calcium retention assay, mitochondrial membrane potential ($\Delta\Psi_m$) changes were followed by a dual-excitation fluorescence ratiometric method (9) with 80 nM tetramethylrhodamine methyl ester, at excitations of 546 and 573 nm, and emission at 590 nm.

Mitochondrial Swelling Assay and Estimation of the Size of the PTP. As before (5), induction of the opening of the PTP with Ca^{2+} was monitored also by following absorbance changes at 540 nm associated with the swelling of mitochondria. In addition, in experiments where HAP1-WT and HAP1-Δ(c+δ) cells were compared, the preparation of digitonin

permeabilized cells included a Benzonase treatment to remove exogenous DNA which otherwise might cause the cells to aggregate and contribute significant signal noise in the absorbance trace. The permeabilized cells (2 x 10^7/ml) were incubated with 1 µl/ml ultrapure Benzonase (Millipore) in the presence of 5 mM $MgCl_2$, at 4°C for 30 min. Then 5 mM EDTA (pH 8.0) was added and the cells were washed twice in cold PBS, and resuspended in swelling assay solutions. The size exclusion limit of the PTP was determined by conducting the mitochondrial swelling assay in the presence of polyethylene glycols PEG 200, PEG 600, PEG 1000, PEG 1500, PEG 2000 and PEG 4000 (10, 11) with a modified assay medium containing 10 mM HEPES, pH 7.2, 215 mM mannitol, 50 mM sucrose and 3 mM KH_2PO_4, in the presence of 5 mM glutamate and 2.5 mM malate, and digitonin-permeabilized cells at a concentration of 1.33 or 2 x 10^7 cells/ml. Sucrose (250 mM) and PEG solutions of equivalent osmotic pressure (12) were added to 30% by volume to the mannitol-sucrose assay medium. The concentrations of the PEGs dissolved in 10 mM HEPES, pH 7.2, were 234 mM PEG 200, 179 mM PEG 600, 144 mM PEG 1000, 109 mM PEG 1500, 89 mM PEG 2000 and 46 mM PEG 4000. These values were derived from polynomial regression fits of curves relating osmotic pressure to solute concentration (12). Experiments were performed at 30°C with stirring, with a 2 min pre-incubation step, and 200 or 300 µM $CaCl_2$ being added after 20 s.

References

1. He J, et al. (2017) Persistence of the mitochondrial permeability transition in the absence of subunit c of human ATP synthase. *Proc Natl Acad Sci U S A* 114:3409–3414.
2. Ran FA, et al. (2013) Genome engineering using the CRISPR-Cas9 system. *Nat Protoc* 8:2281–2308.
3. Essletzbichler P, et al. (2014) Megabase-scale deletion using CRISPR/Cas9 to generate a fully haploid human cell line. *Genome Res* 24:2059–2065.

4. Skehan P, et al. (1990) New colorimetric cytotoxicity assay for anticancer-drug screening. *J Natl Cancer Inst* 82:1107–1112.
5. He J, Carroll J, Ding S, Fearnley IM, Walker JE (2017) Permeability transition in human mitochondria persists in the absence of peripheral stalk subunits of ATP synthase. *Proc Natl Acad Sci U S A* 114:9086–9091.
6. Korge P, Weiss JN (1999) Thapsigargin directly induces the mitochondrial permeability transition. *Eur J Biochem* 265:273–280.
7. Abramov AY, Duchen MR (2003) Actions of ionomycin, 4-BrA23187 and a novel electrogenic Ca^{2+} ionophore on mitochondria in intact cells. *Cell Calcium* 33:101–112.
8. Srere PA, Brazil H, Gonen L (1963) The citrate condensing enzyme of pigeon breast muscle and moth flight muscle. *Acta Chem Scand* 17:S129–134.
9. Scaduto RC, Grotyohann LW (1999) Measurement of mitochondrial membrane potential using fluorescent rhodamine derivatives. *Biophys J* 76:469–477.
10. Pfeiffer DR, Gudz TI, Novgorodov SA, Erdahl WL (1995) The peptide mastoparan is a potent facilitator of the mitochondrial permeability transition. *J Biol Chem* 270:4923–4932.
11. Brustovetsky N, Dubinsky JM (2000) Limitations of cyclosporin A inhibition of the permeability transition in CNS mitochondria. *J Neurosci* 20:8229–8237.
12. Money NP (1989) Osmotic pressure of aqueous polyethylene glycols : Relationship between molecular weight and vapor pressure deficit. *Plant Physiol* 91:766–769.
13. He J, et al. (2018) Assembly of the membrane domain of ATP synthase in human mitochondria. *Proc Natl Acad Sci U S A* 115:2988–2993.
14. Nicholls D, Åkerman K (1982) Mitochondrial calcium transport. *Biochim Biophys Acta* 683:57–88.

15. Brand MD (2005) The efficiency and plasticity of mitochondrial energy transduction. *Biochem Soc Trans* 33:897–904.

16. Haworth RA, Hunter DR (1979) The Ca^{2+}-induced membrane transition in mitochondria. II. Nature of the Ca^{2+} trigger site. *Arch Biochem Biophys* 195:460–467.

17. Massari S, Azzone GF (1972) The equivalent pore radius of intact and damaged mitochondria and the mechanism of active shrinkage. *Biochim Biophys Acta* 283:23–29.

18. Krasilnikov OV, Sabirov RZ, Ternovsky VI, Merzliak PG, Muratkhodjaev JN (1992) A simple method for the determination of the pore radius of ion channels in planar lipid bilayer membranes. *FEMS Microbiol Immunol* 5:93–100.

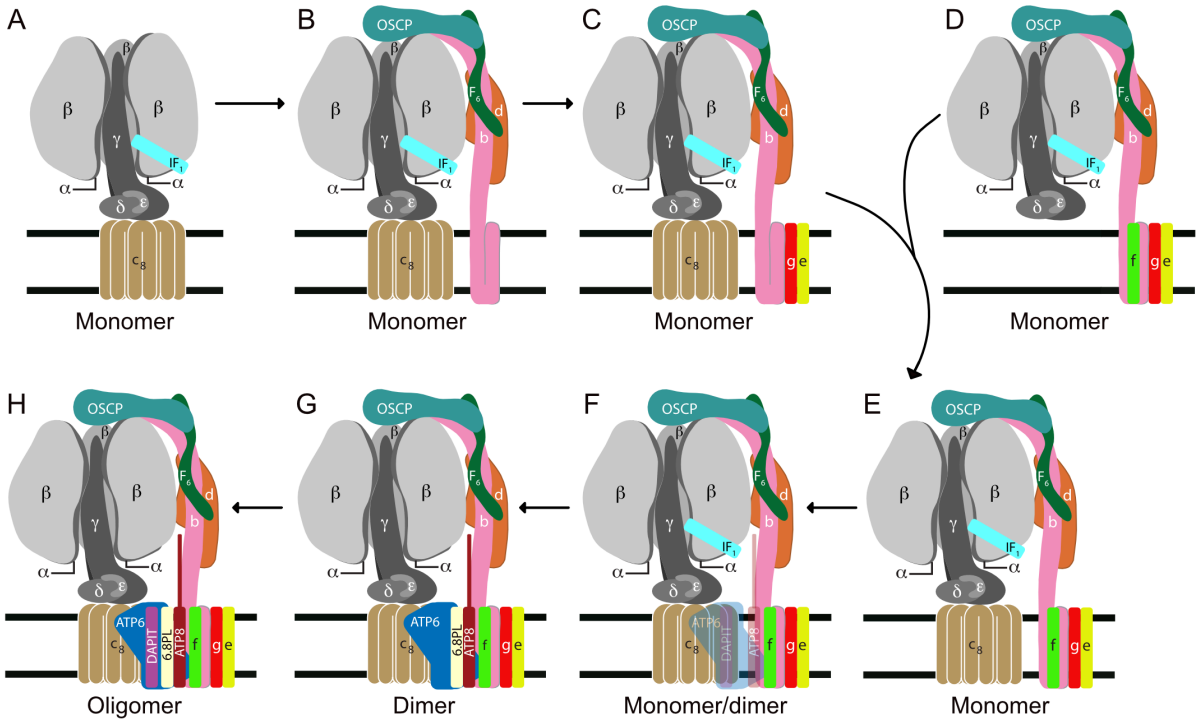

Fig. S1. Pathway of assembly of the membrane arm of human ATP synthase. Parts (*A-D*, *F* and *G*) represent stalled intermediate (or vestigial complexes) characterized from mitochondria of clonal cells with their oligomeric state indicated beneath each panel: (*A*), HAP1-Δb or ΔOSCP; (*B*), HAP1-Δe or Δg; (*C*), HAP1-Δf; (*D*), HAP1-Δc; (*F*), HAP1-6.8PL; (*G*), HAP1-ΔDAPIT. (*E*), vestigial complex from mitochondria of 143B ρ^0-cells. (*H*), the complete monomeric ATP synthase. The horizontal black lines denote the boundaries of the inner mitochondrial membrane. The figure is a modified version of Fig. 6 in ref (13).

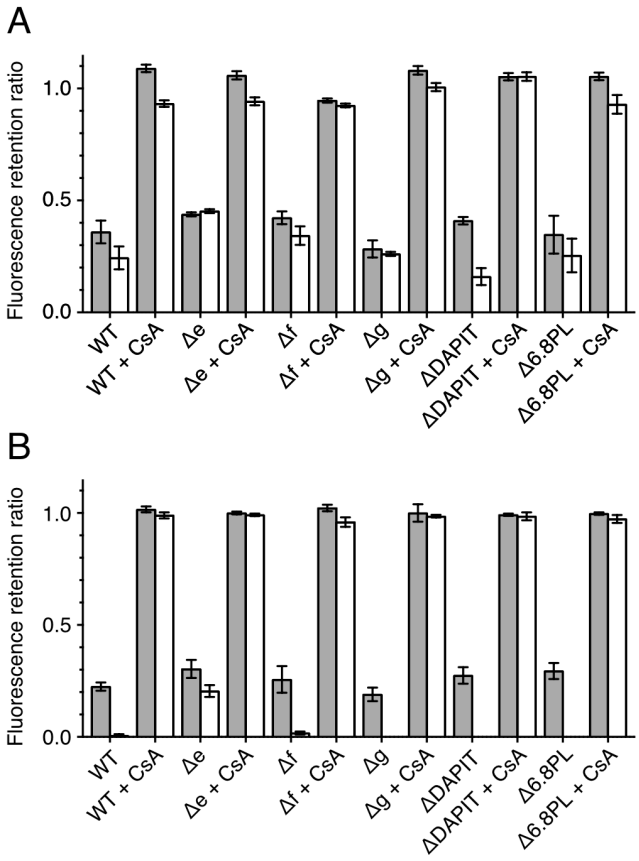

Fig. S2. The opening of the PTP in HAP1 cells. (*A*) PTP opening induced with 40 μM thapsigargin, or (*B*) with 25 μM ferutinin. HAP1-WT, -Δe, -Δf, -Δg, -ΔDAPIT, and -Δ6.8PL cells were stained with calcein and TMRM, and then incubated for 1 h in the presence of 40 μM thapsigargin, or for 30 min with 25 μM ferutinin. Duplicate samples were incubated first in the presence of 5 μM CsA, and then treated with either thapsigargin or ferutinin. Grey and white columns correspond to the fluorescence retention ratios for calcein and TMRM, respectively, compared with cells treated with the vehicle dimethylsulfoxide only. For an example of a scatter plot used in these assays see Fig. S3. The data are mean values ± SDs (thapsigargin, n=2; ferutinin, n=4). For HAP1-Δg, -ΔDAPIT and -Δ6.8PL cells, ferutinin treatment depleted all the TMRM signal from the sampled area. All ratios for ± CsA treatment are significantly different (t-test, $p<0.01$).

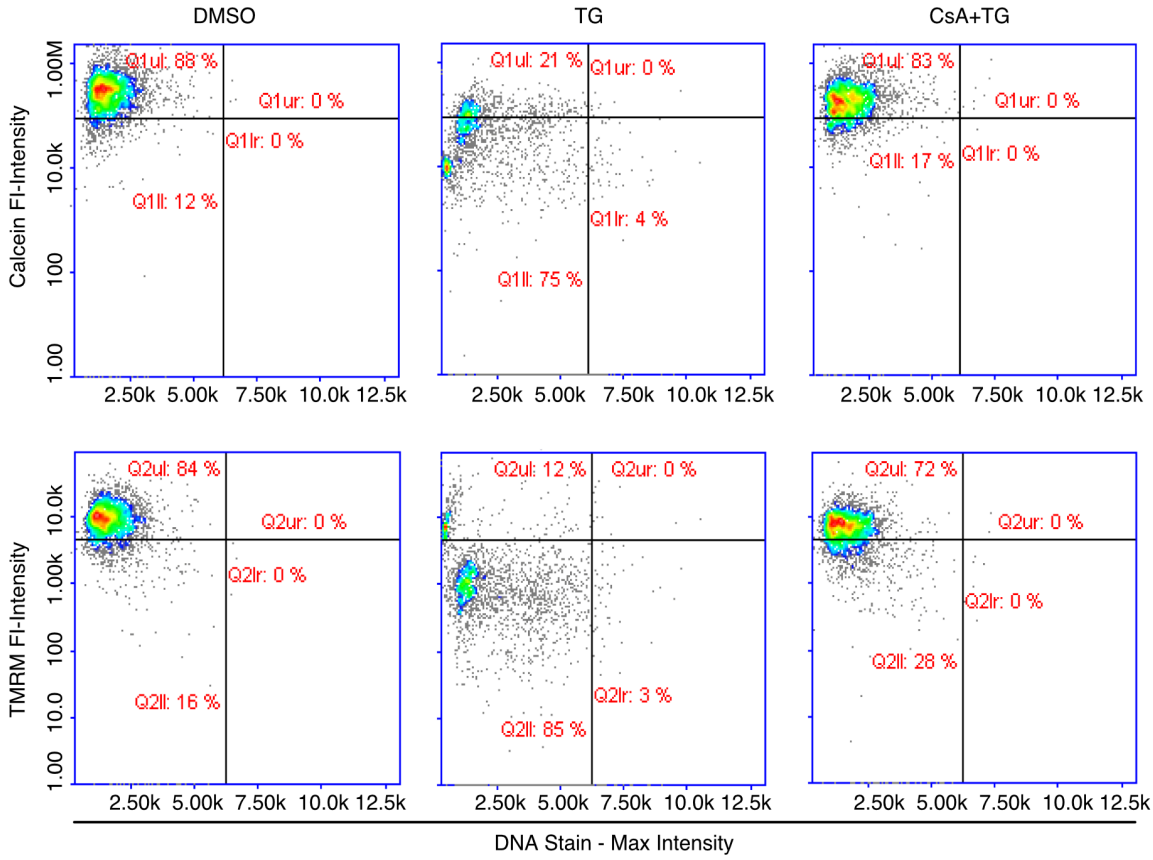

Fig. S3. An example of the scatter plots generated in the assay of the PTP in intact HAP1 cells. HAP1-WT cells were stained with both calcein and TMRM, and then incubated with either 40 μM TG or DMSO vehicle. The fluorescence intensities of calcein and TMRM in samples of cells with or without treatment with TG, and in the presence or absence of CsA, were measured in a Nucleocounter NC3000 cell counting fluorescence microscope (ChemoMetec). Orthogonal axes were drawn manually on the resulting 2D scatter plots for the DMSO treated cells, and then used as the master template for the scatter plots of the treated cells. A relative calcein fluorescence retention ratio of 0.24 after TG treatment was calculated as the ratio of HAP1-WT cell positive percentages (the sum of the two percentages in the upper quadrants (e.g. for calcein and WT plus TG; 21 + 0% = 21%) relative to the positive percentages for WT DMSO treated cells (the sum of the two percentages in the corresponding upper quadrants: 88 + 0% = 88%).

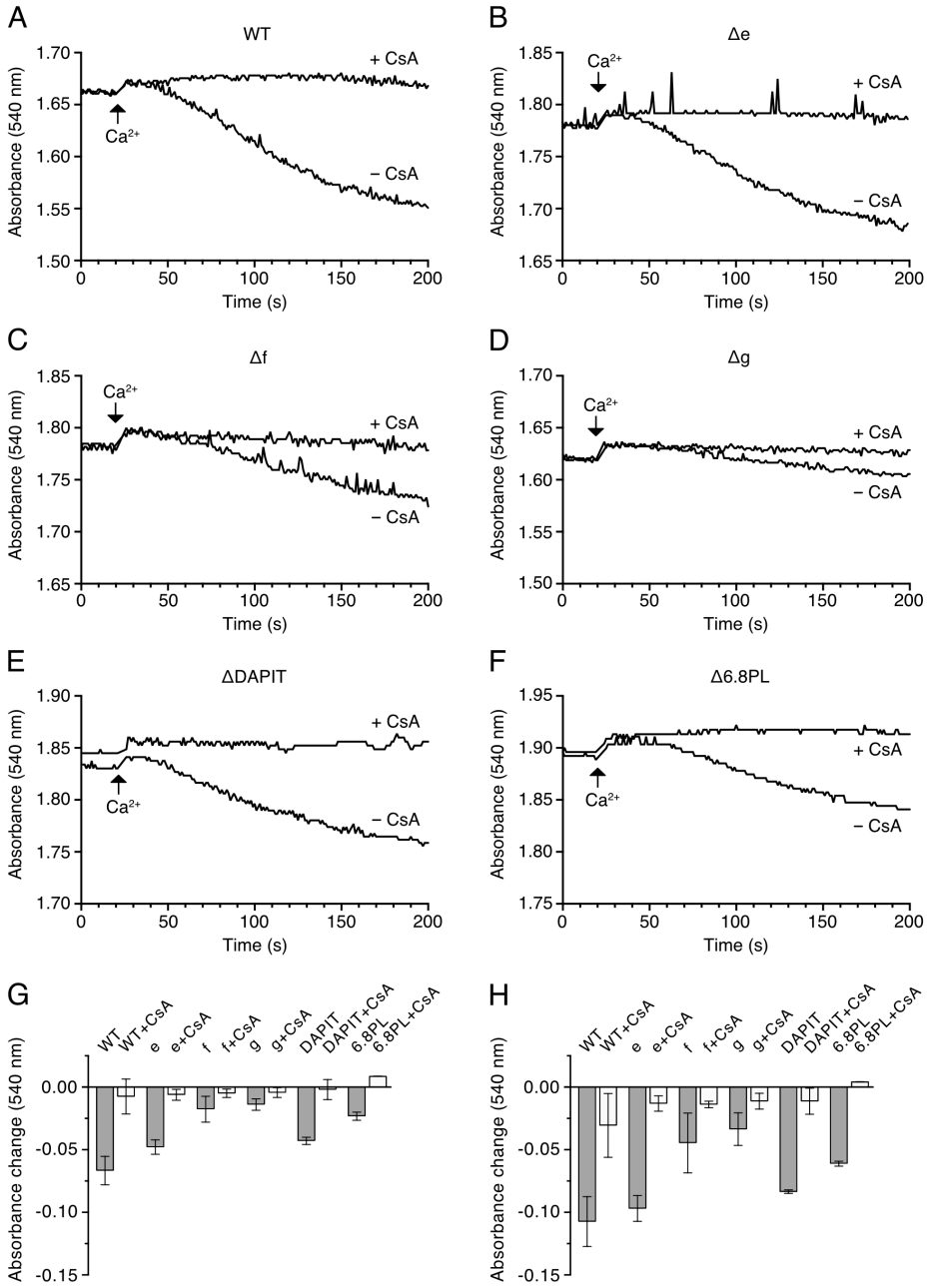

Fig. S4. Effect on light scattering properties of mitochondria in permeabilized HAP1-WT and mutant cells associated with the calcium induced opening of the PTP and swelling of mitochondria. (*A*) HAP1-WT cells; (*B*) HAP1-Δe; (*C*) HAP1-Δf; (*D*) HAP1-Δg; (*E*) HAP1-ΔDAPIT; (*F*) HAP1-Δ6.8PL. PTP opening was induced by the addition of 150 μM $CaCl_2$ to 2 x 10^7 digitonin permeabilized cells/ml. Mitochondrial swelling was monitored in a KCl buffer, by the decrease in absorbance at 540 nm, measured in the presence or absence of 1 μM CsA, and shown with a y-axis scale of 0.2 units for all traces. Initial absorbance values were adjusted to similar levels for comparison. The results show representative data. (*G* and *H*) data showing the average (± SD) absorbance changes at 100 s and 200 s respectively, for WT and mutant cells, relative to the absorbance value at 27 s, corresponding to the peak absorbance immediately after the addition of 150 μM $CaCl_2$ (n = 2 to 6 traces). All data for sample ± CsA, at both points, are significantly different (t-test, p<0.05), except for Δg at 100 s (p = 0.057).

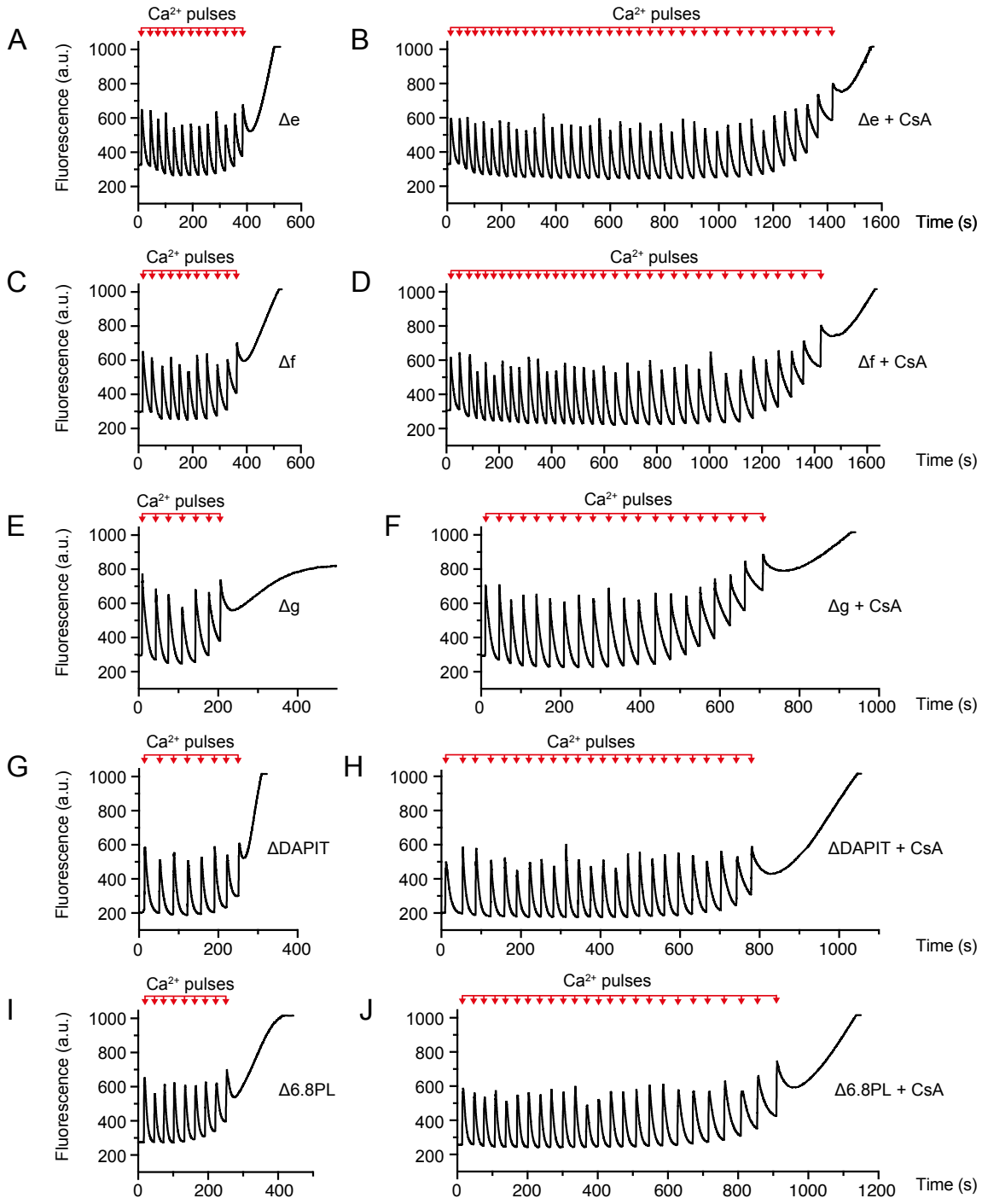

Fig. S5. Calcium induced opening of the PTP in permeabilized HAP1 cells. The calcium retention capacity of mitochondria was determined in digitonin permeabilized cells (2 x 10^7 cells/ml) in response to pulses of 10 µM $CaCl_2$, in the absence and presence of 1 µM CsA. Extra-mitochondrial Ca^{2+} was measured from the fluorescence of Calcium green-5N in arbitrary units (a.u.,). (*A* and *B*), HAP1-Δe cells; (*C* and *D*), HAP1-Δf cells; (*E* and *F*), HAP1-Δg cells; (*G* and *H*), HAP1-ΔDAPIT cells; (*I* and *J*), HAP1-Δ6.8PL cells.

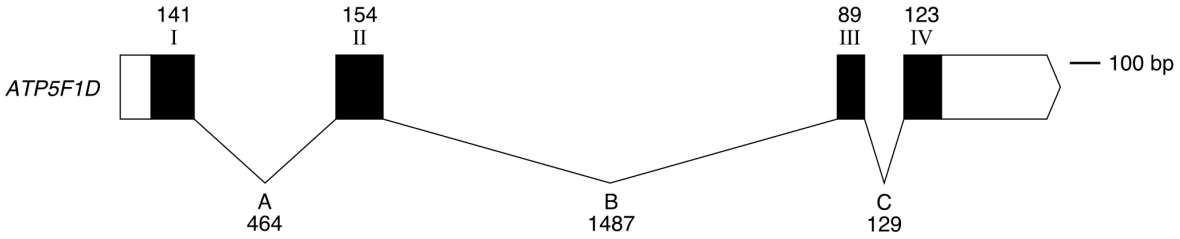

Fig. S6. Structure of *ATP5F1D* encoding the δ-subunit of human ATP synthase. Black and unfilled boxes represent, respectively, protein coding and non-coding regions within exons I-IV. Introns A-C are depicted as intervening continuous lines. Sizes of coding region of exons, and introns are given in base pairs (bp). The exon-intron information was obtained from http://www.ensembl.org and the gene structure of *ATP5F1D* corresponds to reference sequence NM_001687. The images were drawn with the Exon-Intron graphic maker (http://wormweb.org/exonintron).

A

```
                                    ^^^
WT      TGCAGGTCCTGCGGCCGGGGCTGGTCGTGGTGCATGCAGAGGACGGCACCACCTCCAAAT
Δδ      TGCAGGTCCTGCGGCCGGGGCTGGTCGTGGTGCAT-CAGAGGACGGCACCACCTCCAAAT
```

B

```
WT     1 MLPAALLRRPGLGRLVRHARAYAEAAAAPAAASGPNQMSFTFASPTQVFFNGANVRQVDV  60
Δδ     1 MLPAALLRRPGLGRLVRHARAYAEAAAAPAAASGPNQMSFTFASPTQVFFNGANVRQVDV  60

WT    61 PTLTGAFGILAAHVPTLQVLRPGLVVVHAEDGTTSKYFVSSGSIAVNADSSVQLLAEEAV 120
Δδ    61 PTLTGAFGILAAHVPTLQVLRPGLVVVHQRTAPPPNTL---------------------- 98
                               **********

WT   121 TLDMLDLGAAKANLEKAQAELVGTADEATRAEIQIRIEANEALVKALE 168
Δδ    98 ------------------------------------------------  98
```

Fig. S7. Disruption of the δ-subunit of human ATP synthase. CRISPR-Cas9 mediated disruption of the *ATP5F1D* gene was performed in HAP1-A12 cells, in which *ATP5MC1*, *ATP5MC2* and *ATP5MC3* (formerly *ATP5G1*, *ATP5G2*, and *ATP5G3*) had been disrupted previously (1). HAP1-A12 cells are incapable of producing the c-subunit of ATP synthase. (*A*) CRISPR directed 1 bp deletion in exon II of *ATP5F1D* in HAP1-Δ(c+δ) clonal cells. Above the DNA sequence, carets indicate the PAM (protospacer adjacent motif) sequence for the guide RNA, and solid lines the guide RNA target sequence; (*B*) impact of the 1 bp deletion and consequent frame shift on the protein sequence of the δ-subunit. Amino acid changes are indicated by asterisks. A premature stop codon removed residues 99-168 of the mature protein, as denoted by the dashed lines.

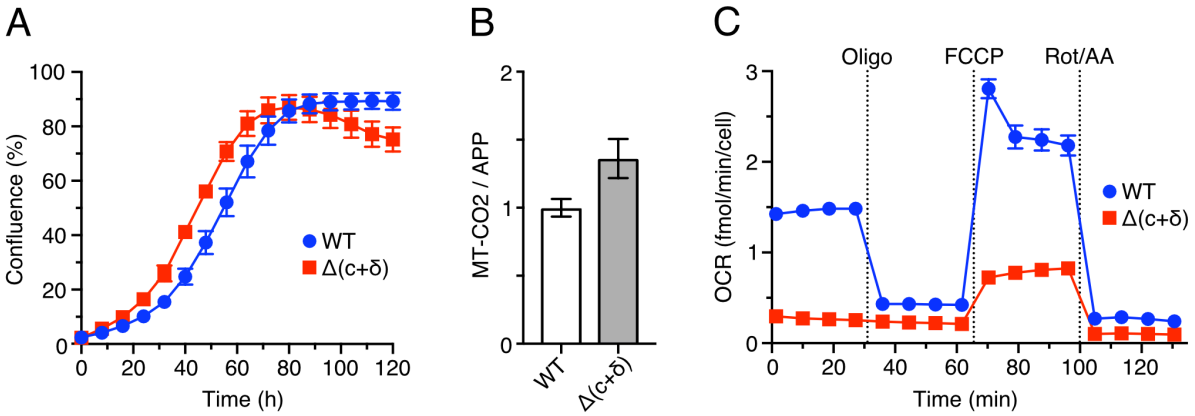

Fig. S8. Characteristics of HAP1-Δ(c+δ) cells. (*A*), Growth rate. About 10^5 cells were seeded into individual wells of a 6-well plate, and their confluence was monitored over 120 h. The data points are the mean values ±SD (n=3); (*B*), relative copy numbers of mtDNA. Regions of the genes *MT-CO2* and *APP* were amplified and quantitated as indices of mitochondrial and nuclear DNA, respectively. All data are the mean values ±SD (n=4); (*C*), cellular oxygen consumption rates (OCR) before and after sequential additions of oligomycin (Oligo), carbonyl cyanide-4-(trifluoromethoxy)phenylhydrazone (FCCP), and a mixture of rotenone and antimycin A (Rot/AA), at the times indicated. Data represent the mean ±SEM (n=10 wells).

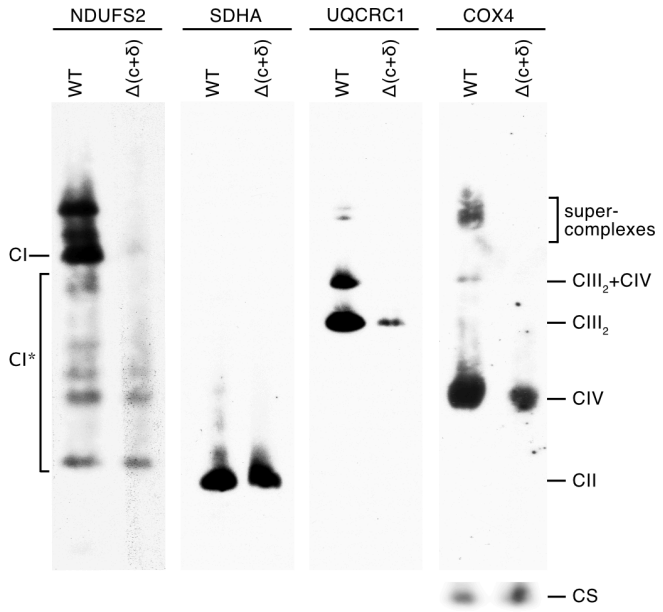

Fig. S9. Assembly of complexes I, II, III and IV in HAP1 cells. Mitoplast samples were prepared from HAP1-WT cells and HAP1-Δ(c+δ) cells, extracted with n-dodecyl-β-D-maltoside (DDM; 3 g/g mitoplast protein), and the extracts were fractionated by BN-PAGE. Complexes were detected by western blotting with antibodies against complex I (NDUFS2), complex II (SDHA), complex III (UQCRC1) and complex IV (COX4). Citrate synthase (CS) provided a loading control. CI, complex I; CII, complex II; $CIII_2$, complex III dimer; CIV, complex IV; $CIII_2$+CIV, complex III dimer plus complex IV; CI*, complex I sub-complex.

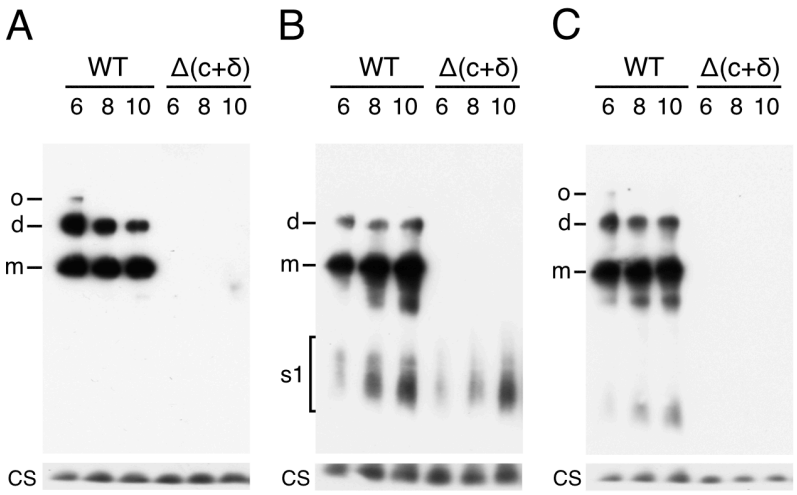

Fig. S10. Oligomeric states of ATP synthase and vestigial forms in HAP1 cells. ATP synthase and vestigial complexes were extracted at the digitonin/protein (g/g) ratios indicated above the lanes, from mitoplasts of HAP1-WT and HAP1-Δ(c+δ) cells. Extracts were fractionated by BN-PAGE, and complexes were revealed by Western blotting with ATP synthase subunit specific antibodies: (*A*), β-subunit; (*B*), g-subunit; (*C*), c-subunit. Citrate synthase (CS) served as a loading control. The positions of the complexes are indicated on the left; d, dimers; m, monomers; o, oligomers; s1, subcomplexes.

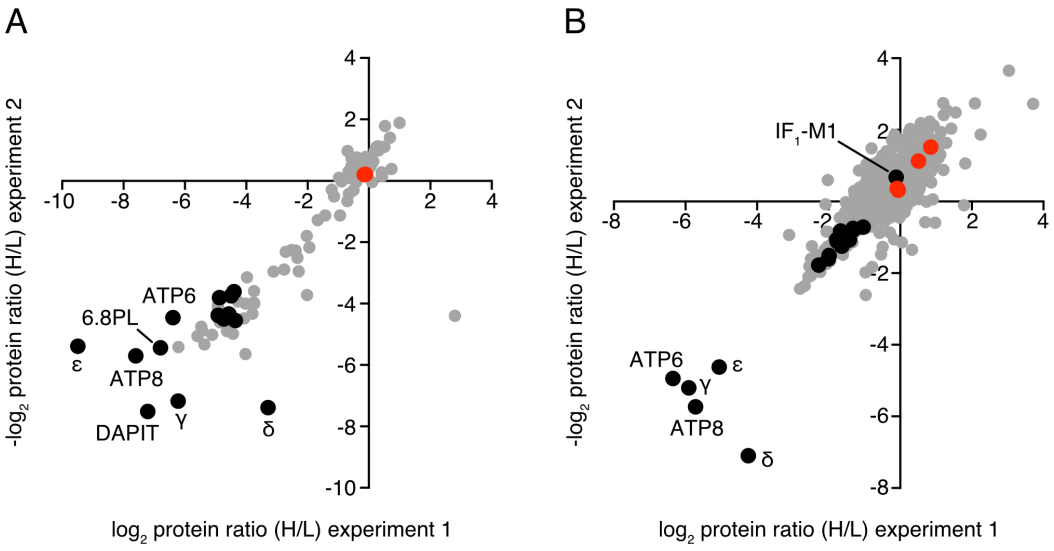

Fig. S11. Relative protein abundances in purified ATP synthase and mitoplast extracts from HAP1-Δ(c+δ) cells. (*A*), immunocaptured ATP synthase; (*B*), mitoplasts. Samples were prepared from a 1:1 mixture of HAP1-Δ(c+δ) cells with HAP1-WT cells that were differentially SILAC-labelled. The experiments were performed twice with reciprocal SILAC labelling orientations. The ratios for proteins obtained in both experiments are plotted as a single point on a scatter plot as the log base 2 value. ●, ATP synthase subunits and forms of IF_1; ●, assembly factors ATPAF1, ATPAF2, C7orf55 and TMEM70; ●, all other proteins. Protein ratios are given in *SI Appendix* Datasets S1-S4.

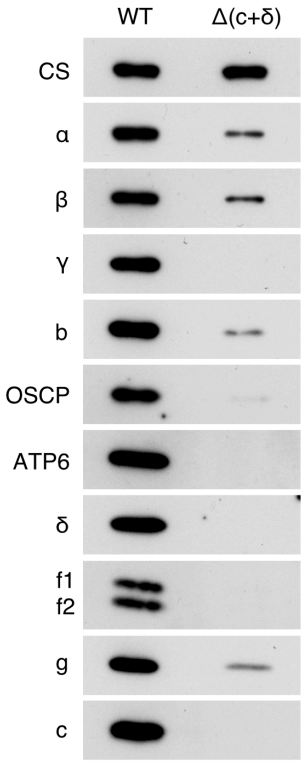

Fig. S12. ATP synthase subunits in mitoplasts from HAP1-WT and HAP1-Δ(c+δ) cells. Mitoplasts were extracted with DDM, fractionated by SDS-PAGE and Western blotted with subunit specific antibodies. Citrate synthase (CS) served as a loading control.

A

Subunit	Δg	Δe	Δf	Δ6.8PL	ΔDAPIT	Δ(c+δ)	Δb	ΔOSCP	Δc
NDUFA7	0.25	0.30	0.43	0.69	0.82	0.17	0.42	0.32	0.25
MT-ND3	0.26	0.34	0.44		0.84				
MT-ND6	0.27		0.43		0.87				
NDUFS4	0.28	0.33	0.42	0.66	0.82	0.18	0.43	0.36	0.28
NDUFA12	0.29	0.34	0.45	0.67	0.83	0.22	0.48	0.54	0.29
NDUFS5	0.29	0.37	0.49	0.65	0.93	0.28	0.56		
NDUFA1	0.31		0.45		0.82		0.58		
MT-ND5	0.32	0.33	0.33	0.64	0.79	0.32	0.51		0.31
NDUFB8	0.33	0.34	0.42	0.59	0.86	0.31	0.57	0.43	0.37
MT-ND1	0.34	0.41	0.48	0.72	0.86	0.42	0.60	0.63	
MT-ND4	0.35	0.39	0.50	0.73	0.85	0.31	0.69		
NDUFB4	0.36	0.42	0.60	0.57	0.96	0.51	0.77	0.93	0.46
NDUFV3_2	0.38	0.47	0.62	0.53	0.96	0.54	1.06	1.18	0.72
NDUFS1	0.39	0.37	0.51	0.59	0.83	0.38	0.66	0.62	0.44
NDUFB7	0.42	0.48	0.51	0.64	0.91	0.49	0.70	0.67	
NDUFC2	0.43	0.47	0.64	0.61	0.91	0.40	0.65	0.53	
NDUFA2	0.44	0.41	0.57	0.62	0.84	0.45	0.74	0.76	0.52
NDUFA10	0.45	0.55	0.68	0.66	0.93	0.46	0.97	1.10	0.50
NDUFB1	0.46	0.54	0.62	0.64	0.89	0.63	0.98	1.00	
NDUFB2	0.46	0.58	0.52	0.78	0.85	0.44	0.92	0.77	
NDUFA11	0.49	0.43	0.59		1.02	0.39	0.68	0.55	
NDUFB9	0.49	0.50	0.54	0.69	0.86	0.46	0.74	0.59	0.50
NDUFC1	0.50				1.00				
NDUFV3_1	0.51	0.41	0.77		0.91				
NDUFV1	0.52	0.55	0.68	0.63	0.88	0.69	0.82	0.97	0.48
NDUFA13	0.56	0.51	0.68	0.62	1.02	0.54	0.87	0.86	0.61
NDUFS6	0.59	0.49	0.74	0.64	0.90	0.48	1.03	1.19	0.52
NDUFV2	0.59	0.64	0.77	0.71	0.91	0.84	0.89	1.18	0.67
NDUFA8	0.60	0.66	0.61	0.77	0.93	0.74	1.06	1.02	0.77
NDUFS7	0.65	0.75	0.78	0.78	0.91	0.66	0.99	1.14	0.73
NDUFS8	0.69	0.82	0.84	0.81	0.89	0.71	1.07	1.12	0.75
NDUFA9	0.72	0.84	0.96	0.93	0.94	0.70	2.71	1.69	0.90
NDUFA3	0.73	0.60	0.78	0.76	1.02	0.71	1.19	1.36	
NDUFS3	0.76	0.87	0.91	0.78	0.90	0.70	1.24	1.35	0.77
NDUFS2	0.76	0.88	0.87	0.80	0.91	0.65	1.19	1.29	0.74
NDUFA5	0.80	0.92	0.92	0.84	0.92	0.76	1.34	1.44	0.78
NDUFB3	0.81	0.80	0.88	0.97	0.93	0.88	1.90	1.86	1.09
NDUFB10	0.82	0.74	0.88	0.73	1.01	1.34	1.86	1.69	1.13
NDUFB5	0.87	0.65	0.81	0.71	1.00	1.25	1.48	1.23	
NDUFB11	0.93	1.01	0.99	0.88	0.96	1.44	2.28	2.06	1.72
NDUFB6	0.99	0.84	1.08	0.81	1.01	1.34	1.82	1.65	1.24
NDUFA6	1.02	0.68	1.06	0.76	0.94	0.88	1.37	1.57	1.03
NDUFAB1	1.14	1.31	1.29	1.08	1.00	1.24	1.34	1.35	

B

Subunit	Δg	Δe	Δf	Δ6.8PL	ΔDAPIT	Δ(c+δ)	Δb	ΔOSCP	Δc
SDHB	0.79	0.84	1.08	1.12	1.04	0.88	0.94	0.91	1.08
SDHD	0.84	1.11	1.27	1.38	1.02	1.24	1.22	1.15	
SDHA	0.84	0.88	1.12	1.16	1.03	1.04	1.06	1.03	1.32
SDHC	0.87	1.05	1.24		1.04	1.09	1.20	1.22	

C

Subunit	Δg	Δe	Δf	Δ6.8PL	ΔDAPIT	Δ(c+δ)	Δb	ΔOSCP	Δc
UQCRB	0.35	0.33	0.46	0.57	0.96	0.23	0.42	0.46	0.25
UQCR11	0.39	0.39	0.54	0.63	0.96	0.24	0.49	0.54	
UQCRQ	0.41	0.40	0.57	0.65	0.94	0.29	0.51	0.62	
UQCRC2	0.45	0.38	0.55	0.56	1.00	0.37	0.58	0.63	0.30
MT-CYB			0.64						
UQCRFS1	0.52	0.54	0.65	0.72	0.96	0.41	0.82	0.83	0.49
UQCRC1	0.54	0.49	0.67	0.62	1.00	0.55	0.85	1.00	0.42
UQCR10	0.88	0.79	0.82	0.94	1.00	1.06	1.35	1.37	
CYC1	0.89	0.82	0.83	0.95	1.05	1.05	1.41	1.34	1.30
UQCRH	0.95	0.96	0.81	0.97	1.02	1.17	1.36	1.29	1.68

D

Subunit	Δg	Δe	Δf	Δ6.8PL	ΔDAPIT	Δ(c+δ)	Δb	ΔOSCP	Δc
MT-CO2	0.26	0.30	0.34	0.63	0.91	0.21	0.50	0.28	0.35
COX6A1	0.29	0.30	0.42	0.60	0.91	0.24	0.58	0.47	
MT-CO1	0.34	0.35	0.39	0.76	0.93	0.29	0.70	0.52	
COX7A2	0.35	0.35	0.46		0.92	0.30	0.70	0.75	
COX7C	0.36	0.34	0.43	0.76	0.91	0.31	0.82	0.68	
COX6B1	0.36	0.35	0.49	0.57	0.99	0.36	0.74	0.92	0.57
COX6C	0.41	0.37	0.51	0.74	0.94	0.41	0.90	0.93	0.55
COX5B	0.45	0.38	0.53	0.79	0.96	0.38	0.82	1.00	0.54
NDUFA4	0.46	0.34	0.50	0.52	1.00	0.35	0.69	0.69	
COX8A			0.46		0.97				
COX4I1	0.58	0.58	0.62	0.91	1.00	0.99	1.42	1.46	1.24
COX5A	0.78	0.85	0.80	1.08	1.03	1.26	1.97	1.86	1.42

Fig. S13. Relative levels of subunits of mitochondrial respiratory chain complexes in HAP1 cells. Mitoplast samples were prepared from a 1:1 mixture of HAP1-Δ(subunit) cells and HAP1-WT cells that were differentially SILAC-labelled. Proteins were fractionated by SDS-PAGE, and stained with Coomassie blue dye. Tryptic digests were analyzed by mass spectrometry. The values are the average of both relative abundance ratios determined for proteins found in the complementary SILAC experiments, normalized to the value for citrate synthase. *A*, complex I; *B*, complex II; *C*, complex III; and *D*, complex IV. The color gradation represents relative values of 0, ; 1, ; maximum, . Gaps are present where insufficient data were obtained to provide ratios for subunits in one or both complementary experiments. No data were obtained for complex I subunits ND2 and ND4L, or complex IV subunits MT-CO3 and COX7B. The data for all of the identified proteins in HAP1-Δ(c+δ) cells are given in *SI Appendix* Dataset S3. Data for HAP1-Δg, -Δe, -Δf, -Δ6.8PL, -ΔDAPIT, -Δb, -ΔOSCP and -Δc cells have been published previously (1, 5, 13).

Table S1. Calcein and TMRM fluorescence retention ratios for HAP1-WT and HAP1-Δ(c+δ) cells treated with ferutinin

	WT						Δ(c+δ)					
	DMSO		-CsA		+CsA		DMSO		-CsA		+CsA	
	Calcein	TMRM	Calcein	TMRM	Calcein	TMRM	Calcein	TMRM	Calcein	TMRM	Calcein	TMRM
	0.90*	0.89	0.16	0.08	0.93	0.86	0.68	0.94	0.21	0.18	0.85	0.89
	0.92	0.90	0.13	0.03	0.94	0.85	0.87	0.88	0.22	0.09	0.78	0.91
	0.92	0.91	0.03	0.06	0.94	0.89	0.79	0.90	0.08	0.03	0.82	0.87
	0.90	0.84	0.02	0.01	0.93	0.83	0.69	0.95	0.12	0.06	0.86	0.87
Average	0.91	0.88	0.08	0.04	0.93	0.86	0.76	0.92	0.16	0.09	0.83	0.88
SD	0.01	0.03	0.07	0.03	0.01	0.02	0.09	0.03	0.07	0.06	0.04	0.02
Ratio†	1	1	0.09	0.05	1.02	0.97	1	1	0.21	0.10	1.09	0.96
Ratio SD‡			0.08	0.03	0.01	0.03			0.09	0.07	0.05	0.02

*Cell percentages are converted to decimal values.

†Average value of the treated cells / average value of the same cells with DMSO treatment.

‡SD, standard deviation of the ratios of individual sample values of the same group.

Table S2. Calcein and TMRM fluorescence retention ratios for thapsigargin treated cells

	WT						Δ(c+δ)					
	DMSO		-CsA		+CsA		DMSO		-CsA		+CsA	
	Calcein	TMRM	Calcein	TMRM	Calcein	TMRM	Calcein	TMRM	Calcein	TMRM	Calcein	TMRM
	0.88*	0.84	0.21	0.12	0.83	0.72	0.88	0.86	0.22	0.27	0.79	0.84
	0.87	0.81	0.21	0.16	0.84	0.78	0.85	0.84	0.22	0.19	0.80	0.73
	0.82	0.86	0.27	0.06	0.88	0.81	0.76	0.83	0.25	0.22	0.79	0.69
	0.85	0.85	0.24	0.05	0.87	0.82	0.84	0.83	0.21	0.16	0.79	0.67
Average	0.85	0.84	0.23	0.10	0.85	0.78	0.83	0.84	0.22	0.21	0.79	0.73
SD	0.03	0.02	0.03	0.05	0.02	0.04	0.05	0.01	0.02	0.05	0.01	0.08
Ratio†	1	1	0.27	0.12	1.00	0.93	1	1	0.27	0.25	0.95	0.87
Ratio SD‡			0.03	0.06	0.03	0.05			0.02	0.06	0.01	0.09

* Cell percentages are converted to decimal values.

† Average value of the treated cells / average value of the same cells with DMSO treatment.

‡ SD, standard deviation of the ratios of individual sample values of the same group.

Table S3. Number of calcium pulses required to open the PTP in permeabilized HAP1-WT cells and in HAP1 mutant cells where individual membrane subunits e, f, g, 6.8PL and DAPIT, or a combination of the δ- and c-subunits have been deleted.

WT			Δe			Δf			Δg			ΔDAPIT			Δ6.8PL			Δ(c+δ)		
CsA*			CsA			CsA			CsA			CsA			CsA			CsA		
−	+	R†	−	+	R	−	+	R	−	+	R	−	+	R	−	+	R	−	+	R
6	17	2.83	13	39	3.00	11	35	3.18	7	20	2.86	8	24	3.00	9	25	2.78	6	16	2.67
4	11	2.75	14	38	2.71	12	33	2.75	6	17	2.83	7	21	3.00	8	28	3.50	3	8	2.67
4	10	2.50	5	16	3.20	10	32	3.20	4	11	2.75	9	18	2.00	7	20	2.86	3	8	2.67
3	6	2.00	5	16	3.20	14	40	2.86	4	10	2.50	9	23	2.56	6	18	3.00	5	15	3.00
9	27	3.00										6	18	3.00	19	43	2.26	5	14	2.80
7	21	3.00																		
9	27	3.00																		
5	13	2.60																		
5	13	2.60																		
5	16	3.20																		
12	44	3.67																		
7	22	3.14																		
5	26	5.20																		
4	18	4.50																		
6	21	3.50																		
5	12	2.40																		

* Experiments were performed in the absence or presence of 1 μM CsA. † Ratio of the number of calcium pulses required to induce the PTP in the presence and absence of CsA.

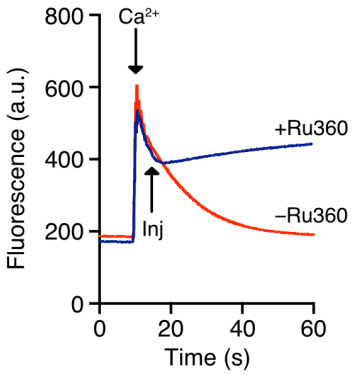

Fig. S14. Inhibition of mitochondrial calcium uptake in HAP1-Δ(c+δ) cells. Digitonin permeabilized cells (2 x 10^7 cells/ml) in a KCl based assay solution containing glutamate and malate were subjected to a single pulse of 10 µM $CaCl_2$, followed by an injection (Inj) of Ru360 (0.5 µM), an inhibitor of the mitochondrial calcium uniporter. Traces with and without Ru360 are shown. Extramitochondrial calcium was measured from the fluorescence of Calcium green-5N.

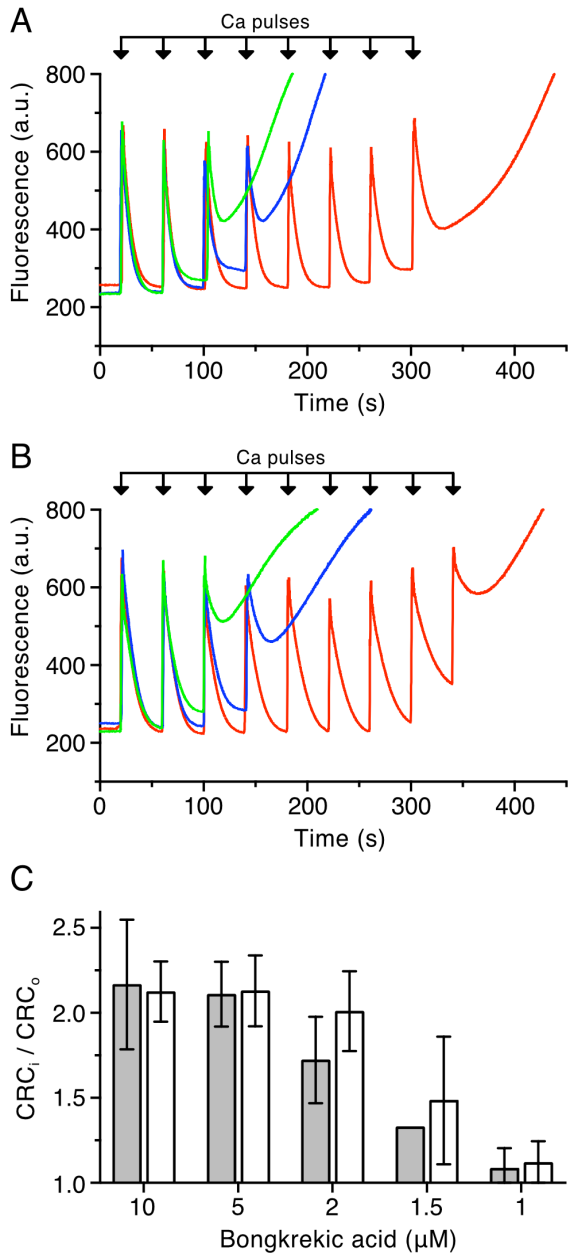

Fig. S15. Effects of bongkrekic acid and carboxyatractyloside on calcium induced opening of the PTP in permeabilized HAP1 cells. The calcium retention capacity of mitochondria of (*A*) HAP1-WT and (*B*) HAP1-Δ(c+δ) cells was determined in digitonin permeabilized cells (2 x 10^7 cells/ml) in response to pulses of 10 µM $CaCl_2$, in the absence (—) and presence of 2 µM bongkrekic acid (—) or 2 µM carboxyatractyloside (—). Calcium uptake by the endoplasmic reticulum was inhibited with thapsigargin (1 µM). Uptake of extra-mitochondrial Ca^{2+} was monitored by the fluorescence in arbitrary units (a.u.) of Calcium green-5N. The collapse of the fluorescence signal corresponds to the opening of the PTP. (*C*) Quantitation of the PTP displayed as the ratio of the number of calcium pulses required to induce the PTP in the presence of bongkrekic acid (CRC_i) to untreated (CRC_o) samples (± SD; n=2 or 3, except for wild-type at 1.5 µM). Gray and white columns correspond to wild-type and Δ(c+δ) cells, respectively.

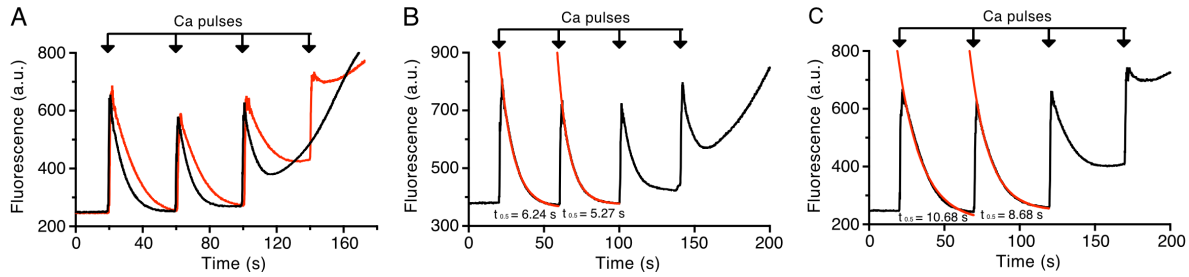

Fig. S16. Comparison of calcium uptake and opening of the PTP in permeabilized HAP1-WT and HAP1-Δ(c+δ) cells. The numbers of HAP1-WT and HAP1-Δ(c+δ) cells were adjusted so that they contained the same amount of citrate synthase. Pulses of 10 µM $CaCl_2$ were delivered to the cells at intervals of 40 or 50 s, and the uptake of extra-mitochondrial Ca^{2+} was followed from the fluorescence of Calcium green-5N measured in arbitrary units (a.u.). (*A*) Overlay of HAP1-WT cells (—) and HAP1-Δ(c+δ) cells (—) pulsed with Ca^{2+} at 40 s intervals. Uptake of calcium into the endoplasmic reticulum was inhibited with thapsigargin (1 µM). The collapse of the fluorescence signal corresponds to the opening of the PTP. A single-phase decay curve (—) was fitted to examples of the calcium uptake trace of HAP1-WT cells (*B*) and HAP1-Δ(c+δ) cells (*C*) using GraphPad Prism software.

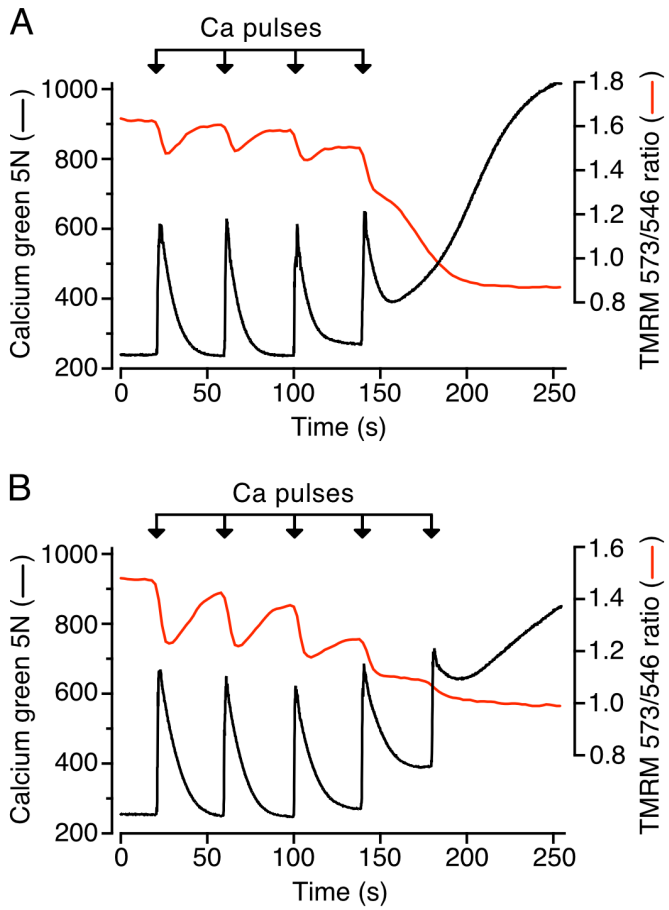

Fig. S17. Mitochondrial membrane potential changes in response to calcium pulses and opening of the PTP. The calcium retention capacity and corresponding membrane potential of mitochondria of (*A*) HAP1-WT and (*B*) HAP1-Δ(c+δ) cells were determined in digitonin permeabilized cells (2 x 10^7 cells/ml) in response to pulses of 10 µM $CaCl_2$. Calcium uptake by the endoplasmic reticulum was inhibited with thapsigargin (1 µM). Uptake of extra-mitochondrial Ca^{2+} by mitochondria was monitored by the fluorescence in arbitrary units (a.u.) of Calcium green-5N. The collapse of the fluorescence signal corresponds to the opening of the PTP. The membrane potential difference across the inner mitochondrial membrane, $\Delta\Psi_m$, was monitored ratiometrically with TMRM (80 nM) with excitation (ex.) at 546 and 573 nm, and emission (em.) at 590 nm (9).

Table S4. Estimated rates of calcium uptake and respiration in HAP1-WT and HAP1-Δ(c+δ) cells. The calculation is based on the half-life of Ca^{2+}-uptake; see for example Fig. S16.

Parameter	WT	Δ(c+δ)
Calcium uptake		
Half-life* (sec)	5.76 ± 0.53 (n=7)	9.86 ± 0.93 (n=8)
Rate† (nmol Ca^{2+}/min/10^6 cells)	2.60	1.52
Required proton extrusion‡ (nmol H^+/min/10^6 cells)	5.20	3.04
Required respiration§ (**A**) (nmol O/min/10^6 cells)	0.65	0.38
Respiration		
Maximal respiration¶ (fmol O_2/min/cell)	2.78 ± 0.58 (n=3)	0.56 ± 0.13 (n=3)
Maximal respiration (**B**) (nmol O/min/10^6 cells)	5.56	1.12
Max respiration (**B**) > Required respiration (**A**)	Yes	Yes

* determined from single exponential fits of the calcium uptake curve after a 10 μM Ca^{2+} pulse (see Fig. S16).

† Rate of calcium uptake determined for the initial half-life.

‡ Accumulation of a Ca^{2+} ion via the MCU is accompanied by the extrusion of 2 protons, and extensive Ca^{2+} uptake requires phosphate (14).

§ Based on a conservative H^+/O stoichiometry of 8 for the electron transport chain and NADH linked substrates, to allow for succinate-linked respiration and proton leak (15).

¶ determined from the average OCR after FCCP treatment, minus the residual OCR after inhibition of respiratory chain activity with a combination of rotenone and antimycin A (see Fig. S8).

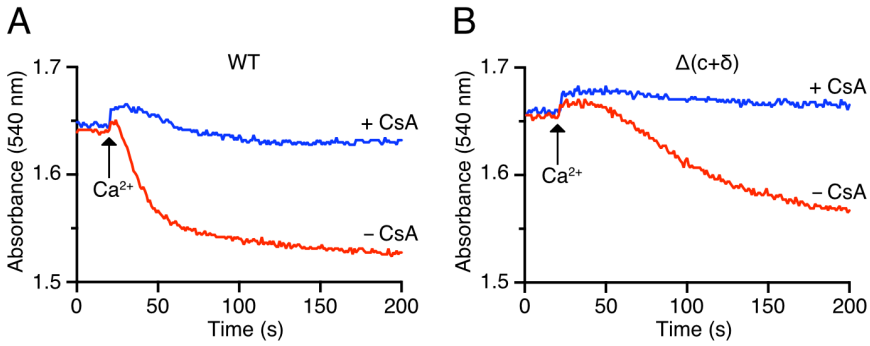

Fig. S18. Calcium induced opening of the PTP and swelling of mitochondria in permeabilized cells. (*A*) HAP1-WT cells; (*B*) HAP1-Δ(c+δ) cells. PTP opening was induced by the addition of 100 µM $CaCl_2$ to 2 x 10^7 digitonin permeabilized cells/ml. Mitochondrial swelling was monitored in a mannitol/sucrose buffer by the decrease in absorbance at 540 nm, measured in the presence or absence of 1 µM CsA. Initial absorbances were adjusted to similar levels for comparison.

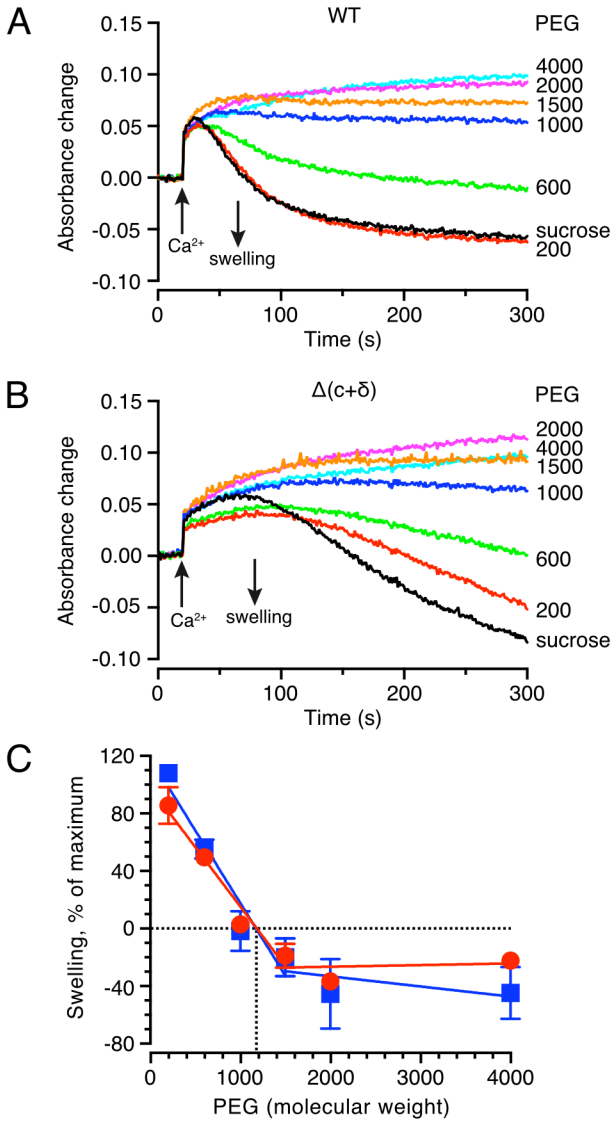

Fig. S19. Size exclusion properties of the PTP in HAP1 cells. Swelling of mitochondria in digitonin-permeabilized cells activated with 200-300 µM Ca^{2+}. (*A*) HAP1-WT cells; (*B*) HAP1-Δ(c+δ) cells. Swelling was monitored by the decrease in absorbance of light at 540 nm, with initial readings adjusted to the same value. Sucrose (250 mM) and polyethylene glycol (PEG) solutions of equivalent osmotic pressure were added to 30% by volume, to the mannitol-sucrose swelling assay medium. Signal drift in the absence of Ca^{2+} (250 mM sucrose with no Ca^{2+} addition) was subtracted from the absorbance changes. (*C*) Absorbances measured after 300 s, expressed as a percentage, relative to the change observed with 250 mM sucrose plus Ca^{2+}. The straight lines (WT, ■; Δ(c+δ), ●) are linear regression fits of the data, for each data set, for PEG 200 to PEG 1500 and separately for PEG 1500 to PEG 4000. Zero % swelling corresponds to a PEG molecular weight of 1175 and 1184 for the HAP1-WT and HAP1-Δ(c+δ) cells, respectively. For HAP1-WT cells, n=2-3, average ± s.d.; for HAP1-Δ(c+δ) cells, n=2-3, average ± s.d.

Table S5. Estimates of the diameter of the PTP permeabilized HAP1 cells compared with the values from various isolated mitochondria.

Method	Parameter	Excluded solute*	Diameter† (nm)	Sample	Reference
PEG exclusion	swelling inhibition	1000-1500	1.9-2.1	permeabilized HAP1 cells	This work
PEG exclusion	swelling inhibition	~3000	2.9	rat brain mitochondria	(11)
PEG exclusion	shrinkage rate‡	~1500	2.1	bovine heart mitochondria	(16)
Polyol exclusion	shrinkage rate‡	> raffinose	≥ 2.8 §	rat liver mitochondria	(17)
PEG exclusion	swelling inhibition	~2000	2.4	rat liver mitochondria	(10)

* Polyethylene glycol molecular weight; † estimated from the hydrodynamic radius of the excluded solute (18); ‡ measured with pre-swollen mitochondria; § estimated from an extrapolation of the curve fit.